



The Mechanism of Surfactant Assisted Dispersion of Single-Walled Carbon Nanotubes in Polyvinylpyrrolidone Solutions

Tennison Yu, Jose Efrain Herrera *

Department of Chemical and Biochemical Engineering, Western University, London, Canada

Email address:

jherrer3@uwo.ca (J. E. Herrera)

*Corresponding author

To cite this article:

Tennison Yu, Jose Efrain Herrera. The Mechanism of Surfactant Assisted Dispersion of Single-Walled Carbon Nanotubes in Polyvinylpyrrolidone Solutions. *Colloid and Surface Science*. Vol. 2, No. 3, 2017, pp. 96-106. doi: 10.11648/j.css.20170203.12

Received: June 9, 2017; **Accepted:** June 26, 2017; **Published:** July 27, 2017

Abstract: Single walled carbon nanotubes (SWNTs) are an extremely attractive material due to their unmatched electronic, mechanical, and thermal properties, however; their hydrophobicity results in strong van der Waals interactions. This, combined with extremely high aspect ratios and flexibility, causes SWNTs to adhere strongly into tightly bundled ropes. In these bundles, SWNTs are not as useful as their linearized unbundled equivalents. In this contribution, the characterization of a system containing SWNTs, cetyltrimonium bromide (CTAB) and the polymer, polyvinylpyrrolidone (PVP) is reported. Results indicate that although individually CTAB and PVP are poor dispersants of SWNTs, together they show a synergic effect. Characterizations studies on the obtained SWNT dispersions suggest that the polymer hydrodynamic radius should have a minimum length that corresponds to intertube separation distance to achieve stable nanotube dispersions and that the effective polymer contact area with the suspended nanotube, rather than the polymer molecular weight regulates ability for SWNT dispersion. The results present a series of considerations that are relevant for the use of polymers as nanotube dispersing agents and an overall facile way of augmenting current dispersion techniques, potentially allowing for increased usage of applications of these versatile materials.

Keywords: Single Walled Carbon Nanotubes (SWNTs), Dispersion, Surfactant, Polymers, Rheology, Cetyltrimethylammonium Bromide (CTAB), Polyvinylpyrrolidone (PVP)

1. Introduction

Part of the fullerene class of nanomaterials, single walled carbon nanotubes (SWNTs) are known to possess superior mechanical, electrical, and thermal properties [1]. This makes them extremely attractive for applications in many different fields across science and engineering. Their potential applications include nano-electrical systems [2] reinforcement for composites [3], diagnostics and drug delivery [4], and catalysis [5]. However, one of the primary challenges in the development of carbon nanotube-based technologies is the inherent difficulty to properly disperse them in hydrophilic environments due to the hydrophobicity of carbon and the subsequent strong van der Waals intertube interactions they experience. This is a significant hurdle because nanotubes show their highest performance potential only when fully dispersed to their highest aspect ratio and

surface area forms.

Several research groups have worked to develop methods to disperse nanotubes in aqueous solutions. One of the most used methods that has been developed involves shearing by ultrasonication followed by either covalent or non-covalent modifications. While both seek to attach a more hydrophilic moiety onto the surface of nanotube, covalent modifications can involve the introduction of functional groups to the nanotube wall, normally carried under severe conditions, which has been shown to potentially damage a nanotubes structure and affect its unique properties. On the other hand, non-covalent modifications use amphiphatic molecules such as surfactants (cationic, anionic, or neutral) or polymers to disperse the nanotubes [6]. Amphiphatic molecules contain both hydrophobic and hydrophilic components – the

hydrophobic component adsorbs to the surface of nanotubes while the hydrophilic component interacts with water. Therefore, without the need to perform destructive chemistry, non-covalent strategies typically preserve the unique properties of nanotubes. This makes the non-covalent strategy generally more favored and there has been an abundance of work done in seeking optimal surfactant or polymer conditions for dispersing nanotubes.

Among non-covalent approaches for SWNT dispersion, several authors have explored the use of a variety of surfactants for nanotube dispersion. For instance, Tan and Resasco used UV-Vis-NIR to evaluate the degree of nanotube dispersions using several surfactants at their listed optimal concentrations in the literature [7]. Compounds containing aromatic moieties seem to consistently lead to better dispersions for SWNTs. This is primarily thought to be due to π - π stacking interactions between π -orbitals of the nanotube and the aromatic ring of the surfactant [7, 8]. Weaker in dispersion ability are alkyl chain surfactants, though if the surfactant contains charged groups these type of surfactants can enhance dispersion through electrostatic repulsion [9]. Surfactants with shorter hydrophobic chains also appear to be more effective at nanotube dispersion. It has been proposed that long chain surfactants would have a harder time penetrating the intertube region of a nanotube aggregate making shorter chains more effective [7] and that ionic surfactants with shorter hydrophobic moieties allow for the surfactant to be readily adsorbed onto the nanotube surface [10]. However the exact mechanism of SWNT dispersion remains elusive. Though it was initially thought that micelles formed on the nanotube surface, more recent evidence indicates that random adsorption of surfactant monomers takes place on the nanotube surface, particularly for alkyl chain surfactants [11].

Polymer-aid SNWT dispersion is another non-covalent strategy for SWNT dispersion. For this specific case, there are currently two main theories on the mechanism of dispersion: wrapping and non-wrapping. The two models differ in the strength of adsorption between the polymer and nanotube. Wrapping occurs when a strong monolayer of polymer adsorbs to and helically wraps a nanotube whereas for non-wrapping, polymers are weakly interacting with the nanotube through Van der Waals forces [12]. Wrapping was first postulated by O'Connell arguing that changes in the length and height distributions of their SDS-dispersed nanotubes seen through atomic force microscopy (AFM) images were consistent with the adsorption of a monolayer of polymer [13]. Maity and collaborators demonstrated wrapping was indeed possible for the case of poly-*N*-vinylcarbazole (PNVC) onto SWNTs and multiwalled carbon nanotubes (MWNTs) [14]. Similarly, Zheng and coworkers used polythymine (T) and found that π - π stacking was a spontaneous process with energies favoring the polymer-nanotube instead of nanotube-nanotube binding [15]. A non-wrapping mechanism has been also observed for the case of nanotubes dispersed with either Gum Arabic (GA) or an alternating copolymer of styrene and sodium maleate

(PSSSty). GA is a highly branched polysaccharide while PSSSty is a linear copolymer of alternating hydrophobic and hydrophilic units [16]. This type of interaction was also reported by Granite and collaborators for SWNT suspension using PVP [17]. Cotiuga also reported a no- wrapping mechanism for the case of carbon nanotubes dispersed using a polystyrene-block-poly (ethylene oxide) polymer [18].

As described above, much work has been done in seeking to understand how different dispersing agents act, however, much of the current research compares these agents one at a time. On the other hand, in most commercial applications carbon nanotubes would likely be incorporated into a multi-component system involving multiple dispersing agents and/or binders. Early studies exploring SWNT dispersion in systems with more than one component include the use of a sodium cholate (SC) - sodium dodecylsulfate (SDS) and a SDS-carboxymethylcellulose system [19]. Additionally, a three-component strategy (hexadecyltrimethylammonium bromide, polyacrylic acid, and polyethylene oxide) has also been tested for the dispersion of nanotubes prior to their incorporation into a SiO₂ ceramic matrix, resulting in different levels of improvement in the mechanical properties of the ceramic [20]. Earlier work by our group, indicated that, compared to SWNT-free chitosan, a polyvinylpyrrolidone centrimonium bromide (PVP/CTAB) system for the dispersion of carbon nanotubes led to a dramatic 20 fold increase in Young's modulus of a SWNT-chitosan matrix [21]. In this contribution, a framework for understanding the mechanism for which this particular surfactant/polymer system (PVP/CTAB) is able to successfully disperse SWNTs. Is presented A combination of characterization techniques including optical spectroscopy, viscosity measurements, surface tension, atomic force microscopy and dynamic light scattering were used. The results show that the PVP CTAB system is synergistic and is ultimately a result of PVP acting through a physical contact mechanism where steric interactions play a fundamental role.

2. Materials and Methods

2.1. Materials

The surfactants, centrimonium bromide (CTAB) and sodium deoxycholate were obtained from Sigma Aldrich (BioXtra). Polyvinylpyrrolidone (PVP) with different molecular weights (10,000 g/mol, 40,000 g/mol, 360,000 g/mol, and 1,300,000 g/mol) were obtained from Sigma-Aldrich as well. PVP at molecular weight of 3,500 g/mol, and 8,000 g/mol were sourced from Acros Organics. From this point onward, the different molecular weights of PVP will be denoted as PVP 3.5, PV 8, PVP 10, PVP 40, PVP 360, and PVP 1300 where the digits correspond to the molecular weight in thousands. Single-walled carbon nanotubes (SWNT) at a purity of >90% (SKU#0101) were sourced from CheapTubes Inc. These materials were used without further purification. GPC chromatography was used to confirm and evaluate the molecular weight distribution of

the PVP polymer (Section 2.2.7).

2.2. Methods

2.2.1. Nanotube Suspension Preparation

CTAB at 0.1% wt/v and PVP of a specific molecular weight at concentrations of 0, 0.25, 0.75, 1.1, 4, 6, 9% wt/v were dissolved together in pure water. From the resulting solution, 25 mL was poured into a 40 mL glass vial containing 5 mg of either nanotubes or fullerenes to bring the carbonaceous compound to a concentration of 0.2 mg/mL. The solution was then mixed via sonication for 2 hours in an ice bath using a Fisher Scientific Model 500 Ultrasonic dismembrator equipped with a step-horn and a half-inch nut. The horn frequency used was about 19.850 – 20.050 kHz. Other settings on the device include 180 W (i.e. 45% amplitude of a maximum of 400 W) and a sonication interval of 0.3 seconds ON and 0.7 seconds OFF. The solution was then centrifuged at 50,000 RPM for 1 hour using a Thermo T-1270 Fixed Angle Titanium Rotor placed in a Sorvall WX series ultracentrifuge to separate dispersed and undispersed nanotubes. Lastly, the top half of the resulting supernatant was filtered through 2 pieces of Whatman Grade 1 Qualitative Filter Paper to remove any large undispersed solids.

2.2.2. Spectroscopic Characterization

Optical absorption spectra of the samples were obtained using a Shimadzu UV-3600 from wavelengths of 400 nm to 1,400 nm with a slit width of 8.0 and a medium scan speed. The contents of the blanks of all nanotube dispersions were of the same material and concentrations of the samples themselves without the nanotubes present in solution. The dispersion area was then analyzed using Origin 8.5 s Peak Analyzer tool whereas the total area under the curve was analyzed with the Integration function available in the same program.

2.2.3. Atomic Force Microscopy

To obtain images of nanotube distributions for length and radius, 20 μL of sample was pipetted onto a cm^2 of silicon wafer and spread into a thin film using a disposable cell spreader. The wafer was then heated at approximately 185°C for 4 hours followed by a wash with 1.5 mL of pure water and dried again at the same temperature for 10 minutes. They were then brought to the atomic force microscope (AFM, Dimension 3100, Veeco Inc) for imaging. All images were captured under tapping mode with a silicon nitride cantilever with a nominal spring constant of 40 N/m and a tip radius of around 10 nm. Distributions from the images were then processed using the Gwydion software.

2.2.4. Dynamic Light Scattering (DLS)

This technique was used to determine and verify the size distribution of the particles within the solutions. All samples were prepared at a polymer concentration of 1.1% wt/v or less through simple mixing and diluting. This was done to avoid any significant viscosity changes which would effect results automatically calculated by the instrument software.

The samples were then filtered using 2 pieces of Whatman Grade 1 Qualitative Filter Paper to remove large dust particles. Samples were then transferred into a cuvette and placed inside Brookhaven's ZetaPlus Zeta Potential Analyzer. Using the BIC Particle Sizing program (which runs Brookhaven's MAS OPTION software), 10 runs of each sample were analyzed at a temperature of 25°C, angle of 90°, and a wavelength of 659 nm. The run time of each experiment varied between samples and was set to the amount necessary to obtain a suitable exponential decay autocorrelation curve. The Multi-modal Size Distribution (MSD) analysis tool which uses the non-negative least square (NNLS) algorithm was then used to resolve multimodal particle distributions.

2.2.5. Surface Tension Measurements

Surface tension measurements were carried using a First Ten Angstroms 1000 B Class contact angle and surface tension instrument. The corresponding software, FTA 32, can be used to capture images and automatically uses the Young-Laplace equation relating interfacial tension to a drop shape produced at the end of a needle. Before each sample was analyzed, 0.5 mL of it was sacrificed for rinsing of the needle to minimize contamination. Afterwards, sufficient amounts of the sample was aspirated and the needle which had a blunt ended bevel was then loaded onto the machine apparatus. For each sample, several pictures were taken to avoid error that may occur from asymmetrical droplet formation which can cause minute errors in the determination of surface tension. After each sample, the needle was rinsed with pure water and compressed air was gently flowed through it to ensure no dilution when rinsing with the next sample. To obtain values such as the CMC, two lines were firstly drawn at regions of linearity: one with decreasing points of surface tension indicating the saturating droplet surface and the other with points after the surface droplet had saturated with the surfactant. The intersection of these two lines was determined to be the critical micelle concentration (CMC). The 95% confidence interval (CI) of the CMC values were calculated using previously reported methodology [22].

2.2.6. Viscosity Measurements

To obtain viscosity values, 1.5 mL of the samples were placed onto the stage of an AR 1500 EX rheometer. A 40 mm 4° steel cone was lowered to a gap height of 162 μm and the sample was subjected to steady state flow tests with a shear rate ramp from 0.02864 s^{-1} to 2,000 s^{-1} in a logarithmic step. Viscosity values were taken at 25°C under Newtonian behavior.

2.2.7. Gel Permeation Chromatography (GPC)

To ensure the quality of the PVP from suppliers, samples were sent to PolyAnalytik in London, Ontario, Canada. Their procedure involved analysis using 3 methacrylate-based gel columns PAA-206M, PAA-203, PAA-202 in a mobile phase of 0.1 M NaNO_3 on a Viscotek Tetra Detector Array at a flow rate of 0.5 mL/min and a temperature of 30°C. The Tetra Detector Array included a Refractive Index detector (660 nm

LED), UV detector (Deuterium lamp), Light Scattering detector (670 nm laser, 7° and 90° degrees) and Viscometer detector (four-capillary bridge). The samples were dissolved in pure water and shaken overnight. The samples were filtered either through a 0.2 µm (PVP samples) or a 0.45 µm (nanotubes) Nylon filter before injection. The injection volume used was 100 µL-150 µL. For polymer samples, a combination of the Refractive Index and Light Scattering detector were used to determine the molecular mass while the Viscometer detector was used to determine the hydrodynamic radius. The results obtained are shown in Table 1. For samples containing SWNT, a combination of the Refractive Index and UV detectors were used. These results are shown in Table 2.

3. Results

3.1. SWNT Dispersion Characterization

Vis-NIR spectroscopy was used to characterize nanotube dispersion. This technique was chosen to take advantage of the unique electronic band structure of nanotubes. Nanotubes

of different diameters and chiralities have distinct electronic structures and thus would lead to optical absorption spectra with different absorption bands. In a sample with nanotubes of different diameters and chiralities, the optical absorption bands overlap and create a convoluted distribution of peaks. The resolution of the peaks is strongly dependent on how well dispersed the nanotubes are in solution. Nanotubes that are aggregated in bundles generally give poorly resolved spectra because of light scattering by the nanotube bundles. Therefore, a well dispersed sample would result in spectra with sharp resolved peaks in the Vis-NIR region, these peaks are linked to van Hove transitions and represent the quantization of the density of states of the SWNTs [23]. These peaks can be integrated with respect to the scattering background, since an increase in these area values is indicative of a greater degree of dispersion. To quantify the degree of nanotube dispersion, the area under the van Hove peaks observed in the Vis-NIR spectra were taken relative to a localized scattering baseline (non-resonant background). A detailed description of this methodology has been previously published [21].

Table 1. Summary of GPC results for the analysis of PVP materials of different molecular weight.

Nominal molecular weight of polymer sample	Peak Ret. Vol. (mL)	Mn (g/mol)	Mw (g/mol)	Mz (g/mol)	Intrinsic viscosity (dL/g)	Hydrodynamic radius (nm)
3500	22.414	1,551	3,527	6,296	0.05	1.3
8000	21.723	3,568	8,009	14,720	0.07	1.9
10,000	23.694	4,359	14,171	37,087	0.08	2.4
40,000	22.373	21,516	53,200	131,185	0.20	5.1
360,000	19.731	279,736	803,087	2,128,000	1.26	22.9
1,300,000	19.862	240,318	605,688	1,395,000	1.13	20.4

Table 2. Summary table of GPC results for a SWNT dispersed in a solution of 0.75% PVP 10, 0.1% CTAB. The nanotube nominal concentration is 0.2 g/L SWNT.

	Peak Ret. Vol. (mL)	Mn (g/mol)	Mw (g/mol)	Mz (g/mol)	IV (dL/g)	Concentration (mg/mL)
Peak 1	18.153	358,736	646,103	1,020,000	15.526	0.027
Peak 2	23.837	6,056	12,696	28,583	0.0761	7.959

Results of previous research indicate that the surfactant centrimonium bromide (CTAB) and polyvinylpyrrolidone (PVP) at 10,000 g/mol are able to disperse nanotubes in aqueous solutions [21]. To validate this experimental methodology, 5 mg of SWNT were placed in 25 mL of 0.1% wt/v solution of CTAB and/or 6% wt/v PVP 10, ultrasonicated to mix, and ultracentrifuged to remove impurities to ultimately achieve the dispersed sample. Figure 1 provides the obtained spectral profile for the three samples. The presence of peaks in the resulting spectra is indicative of the dispersion quality of the obtained nanotube suspension. By integrating with respect to the resonant area, as previously described²¹, a total value of approximately 26.8 was found for SWNT dispersion prepared using CTAB alone, 6.34 for

SWNT dispersion using PVP 10 alone, and 94.3 for a SWNT dispersion prepared using both CTAB and PVP 10 together. Quite noticeably, there is almost a 3-fold increase compared to 0.1% wt/v CTAB alone and almost a 9-fold increase compared to 6% wt/v PVP 10 alone when both CTAB and PVP 10 are combined. From this dramatic increase, the effect appears synergistic and not additive. To gain a better understanding on how the concentration and molecular weight of polymer affects the resonant area, and thus SWNT dispersion, SWNT suspensions were prepared using CTAB 6% PVP, using PVP materials with different molecular weights: 3,500 g/mol, 8,000 g/mol, 40,000 g/mol, 360,000 g/mol, and 1,300,000 g/mol. These results obtained for resonant area are shown in Figure 2.

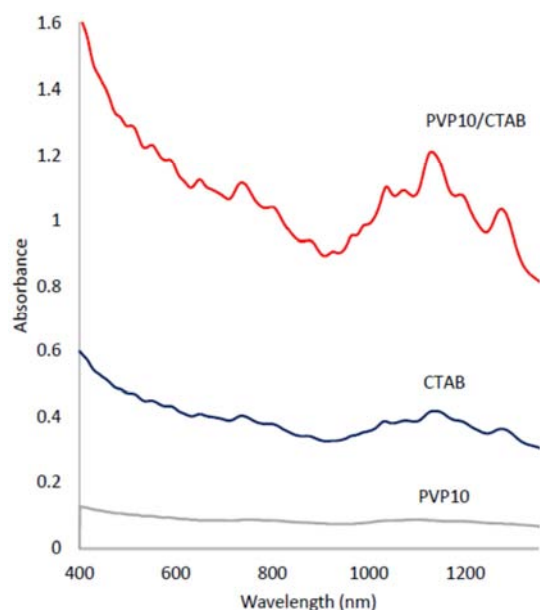


Figure 1. Optical absorption spectra obtained on SWNT suspensions prepared using 6%wt./vol PVP (MW: 10,000), 0.1% wt./vol CTAB, and a combined mixture of 0.1%CTAB and 6% PVP (MW: 10,000) (wt./vol).

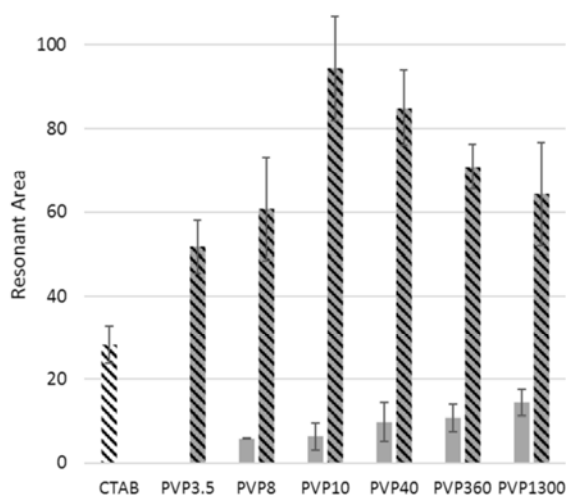


Figure 2. Optical absorption resonant area obtained on SWNT dispersions prepared using 0.1% wt/vol CTAB (transparent background with diagonal stripe pattern), 6%wt./vol PVP of different molecular weights (grey bars) and a mixture of 0.1% wt./vol CTAB and 6%wt./vol PVP of different molecular weights (grey background with diagonal stripe pattern).

Figure 2 clearly shows the dramatic increase in resonant area observed in all case where both the surfactant and the polymer are present. Compared to the case of CTAB/PVP 10 increasing or decreasing the polymer molecular weight resulted in poorer dispersions relative to PVP 10 however the synergic effect remains. For comparison purposes, a semiquantitative scale was developed where the resonant area values obtained are divided by the resonant area value calculated for the case of a SWNT suspension obtained using a PVP-free CTAB solution. This ratio is presented as “percent improvement in dispersion” generated by the presence of the PVP polymer. The values thus obtained are shown in Figure 3.

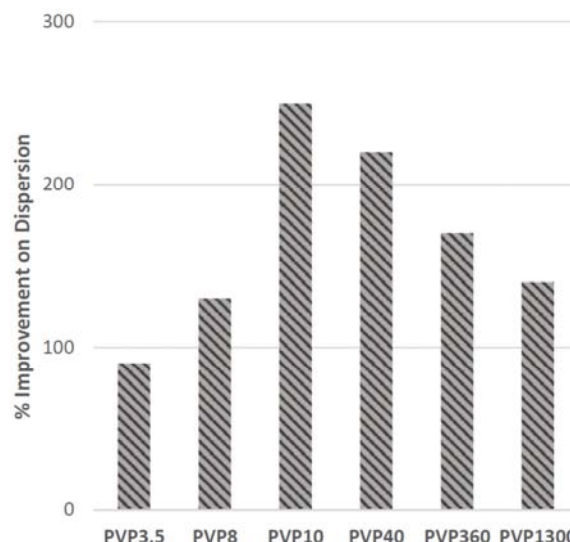


Figure 3. Percentage on improvement in dispersion respect to CTAB alone observed on SWNT suspensions prepared using 0.1% wt./vol CTAB and 6%wt./vol PVP of different molecular weights.

To gain a better understanding on how the addition of polymer affects the resonant area, several different concentrations of PVP at different molecular weights were tested. SWNT dispersions were thus prepared at the additional concentrations of 0.25% wt/v, 0.75% wt/v, 1.1% wt/v, 4% wt/v, and 9% wt/v with each molecular weight. The values obtained on dispersion improvement are shown in Figure 4 as a function of PVP content on the SWNT suspension. These results show a consistent increase in SWNT dispersion with increasing polymer concentration for all PVP molecular weights tested. Among all PVP molecular weights tested PVP 10 (MW = 10,000) gives the best dispersion, PVP 40 (MW = 40,000) also resulted in a moderately successful dispersion though as not as good as the one obtained using PVP 10. All other PVP molecular weights such as the smaller PVP 3.5 and PVP 8, and the larger, PVP 360 and PVP 1300 resulted in relatively poor dispersion profiles. Since polymers of different sizes affect viscosity differently, it was also important to assess dispersion in this regard and to evaluate if the variances in dispersion ability are entirely due to viscosity differences a cone and plate rheometer was used to determine the viscosity of each solution. Once viscosity values were obtained, the percent improvement in dispersion of each sample was replotted against its solution viscosity, these results are shown in Figure 5. A quick inspection of the graph obtained indicates that viscosity does indeed play a role in dispersing nanotubes. The general trend is that an increase in viscosity results in better SWNT dispersions. However, the molecular weight of the polymer itself, and therefore its size, plays a larger role in nanotube dispersion than viscosity does. For instance, for viscosity values near 2.2 mPa. sec, PVP 10 (squares) is a better dispersant than PVP 40 (diamonds) and PVP 8 (filled circles).

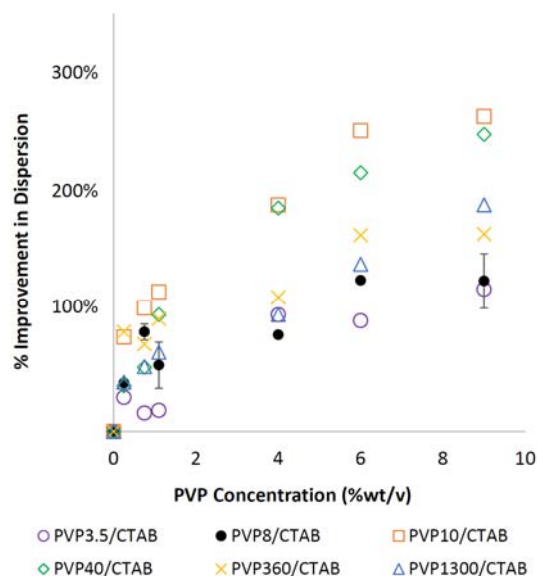


Figure 4. Percentage on improvement in dispersion respect to CTAB alone observed on SWNT suspensions prepared using 0.1% wt./vol CTAB and PVP of different molecular weights (\circ PVP 3,500; \bullet PVP 8,000; \square PVP 10,000; \diamond PVP 40,000; \times PVP 360,000; \triangle PVP 1,300,000) at different PVP concentrations (0.1-10%wt./vol).

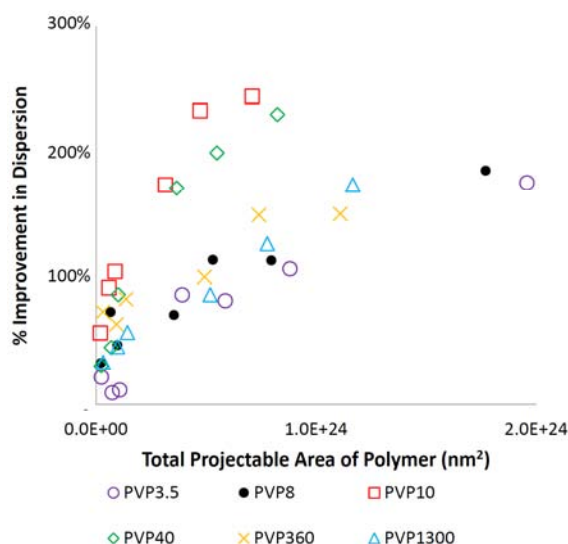


Figure 5. Percentage on improvement in dispersion respect to CTAB alone observed on SWNT suspensions prepared using 0.1% wt./vol CTAB and PVP of different molecular weights (\circ PVP 3,500; \bullet PVP 8,000; \square PVP 10,000; \diamond PVP 40,000; \times PVP 360,000; \triangle PVP 1,300,000) at different concentrations as a function of dispersant solution viscosity.

Another interesting trend observed in Fig. 5 is the presence of two distinct regions where the dispersion quality dependence on viscosity follow different profiles. Specifically, for all PVP molecular weights tested, from 1 to 2 – 3 mPa·sec. the dispersion ability of the combined CTAB/PVP system follows a sharp linear dependence on viscosity. In contrast for viscosity values above to 2 – 3 mPa·sec. there is almost a negligible improvement in dispersion quality as viscosity increases. To understand these two distinct trends, the values for polymer intrinsic viscosity (calculated using the GPC data (Table 1) were used in combination with Equation 1 to calculate the polymer overlap concentration (C^*):

$$C^* = \frac{0.77}{[\eta]} \quad (1)$$

The polymer overlap concentration is the minimum concentration at which polymers are abundant enough in solution to allow for polymer chains to begin crossing with each other, this value is characteristic for each polymer and heavily dependent on molecular weight and degree of branching [24, 25]. The values thus obtained are shown in Table 3. The calculated determined overlap concentrations are consistent with similar values previously reported in the literature [26-28] (also shown in Table 3). As expected the overlap concentrations are larger at low molecular weights.

To further rationalize the results shown in Figure 5 a value for an “overlap viscosity” was calculated. The overlap viscosity if defined in this work as the experimental value obtained for viscosity at overlap concentrations. The values obtained are reported in Table 3 as well. The data clearly indicates that in the 2 – 3 mPa·sec viscosity range where PVP molecules begin to overlap. Therefore, it can be proposed that the ability of PVP to disperse SWNTs is significantly linked not to a change of viscosity of the system, but possible to a steric effect since once the polymer chains start overlapping with each other there is only a slight improvement in SWNT dispersion. Surface tension tests were carried as well to investigate whether PVP presence and concentration affects the behavior of CTAB. In particular, CTAB’s critical micelle concentration (CMC). No significant changes in the CMC values were observed for all solutions containing PVP for at various molecular weights and concentrations.

Table 3. Overlap Concentrations and corresponding overlap viscosity for PVP of different molecular weights as estimated using GPC data and Equation 1.

Polymer	Overlap Concentration (% wt/v)	Overlap Viscosity (mPa·sec)	Overlap concentration from literature (% wt/v)
PVP 3.5	14.53	2.50	-
PVP 8.0	13.28	3.01	-
PVP 10	9.28	2.44	-
PVP 40	3.91	2.12	3.21 (MW: 30 k), 2.14 (MW: 55 k) ref. [27]
PVP 360	0.61	2.06	1.22 (MW 310 K) ref. [28]
PVP 1300	0.68	2.35	0.79 (MW 1300 K) ref. [26]

3.2. Atomic Force Microscopy

Many researchers previously reported that nanotubes can be fragmented during ultrasonication resulting in nanotubes with smaller lengths [29, 30], which are then easier to disperse. To assess whether this was a phenomenon occurring within the system presented in this study, AFM was used to evaluate the length and diameter distributions of nanotubes in the dispersed samples. A solution containing 0.1% wt/v CTAB and 0.2 g/L SWNT was aliquoted onto a polished silicon wafer, dried at 180°C, washed profusely with pure water to remove surfactant molecules, and dried once more

before immediately being analyzed on the AFM. This sample was chosen, instead of those containing polymers, to avoid misinterpretation due to polymers deposition on the solid substrate. Since this sample was sonicated using the same protocols consistently used for all samples in this study, it was assumed that any disruption of the nanotube geometric structure potentially observed would be representative of all samples in this study. From the acquired AFM images, the diameter and length of the observable strands were subsequently measured using the software, Gwyddion®. The results obtained are presented in Table 4.

Table 4. Summary of frequency distribution of nanotube diameter, length, and calculated molecular weight as obtained from AFM.

Diameter (nm)	Frequency	Length (nm)	Frequency	Molecular Weight ($\times 10^6$ g/mol)	Frequency
< 1	5	< 200	4	< 0.5	5
1 – 2	25	200 – 400	9	0.5 – 1.0	14
2 – 3	21	400 – 600	25	1.0 – 1.5	12
3 – 4	10	600 – 800	10	1.5 – 2.0	6
4 – 5	4	800 – 1000	5	2.0 – 2.5	10
> 5	1	1000 – 1200	6	2.5 – 3.0	3
		1200 – 1400	4	3.0 – 3.5	1
		> 1400	3	3.5 – 4.0	6
				4.0 – 4.5	3
				4.5 – 5.0	1
				> 5.0	5

The obtained histograms indicate that after sonication most nanotubes have a diameter between 1 nm - 2 nm and a length of about 400 nm - 600 nm. Using these dimensions, a molecular weight distribution of about 500,000 – 1,000,000 g/mol (assuming 100% carbon) was also calculated stoichiometrically by using a density of 1.33 g/cm³, following the methodology of Hadjiev and collaborator [31]. The observed outer diameter and length were in range of those found in literature in which sonication was part of the dispersion methodology [15, 23, 32, 33]. The DLS results (not shown) on the samples obtained are also in agreement with these AFM results. It was also observed that the molecular weight of nanotubes obtained using GPC (646 100 g/mol, Table 2) falls within the expected range calculated using the AFM data.

4. Discussion

Initial sample preparation using only 0.1% wt/v CTAB to disperse nanotubes resulted in a relatively stable suspension in which nanotubes were appreciably dispersed. The optical absorption measurements on this sample indicated an acceptable level of SWNT dispersion in aqueous solutions. Suspensions prepared using PVP 10 as dispersing agent, in the absence of CTAB, resulted, in contrast, in poor SWNT dispersions. On the other hand, the addition of PVP to a system already containing CTAB resulted in an unexpected synergism that resulted on a marked improvement of the level of SWNT dispersion. This phenomenon was most prominent when PVP 10 was used as higher and lower PVP molecular weights were not as effective (Fig. 3).

Probing the system using AFM and DLS to observe any changes in dimensionality of the system components showed

that the nanotube had been fragmented likely due to ultrasonication, as previously reported [30]. Checking for changes in the behavior of CTAB in the presence of PVP using surface tension measurements also revealed no significant changes with regards to the formation of micelles or the behavior of CTAB in general. This is consistent with earlier observations, indicating that cationic surfactants could interact with PVP only at pH values above 11, [34] and previously reported results demonstrating that CTAB and PVP do not directly interact with one another [35-37]. Thus, based on these surface tension measurements and literature reports, it is possible to postulate that CTAB and PVP do not substantially interact.

Given the hydrophobic (SWNT) and hydrophilic (PVP) properties of the system macromolecules it is plausible to assume that the hydrophobic ends of CTAB adsorbs to the surface of the nanotubes. Qi and collaborators have previously reported full nanotube aqueous saturation at 0.075 g/L SWNT when using a CTAB concentrations of 1 mM (0.036% wt/v) [38]. Therefore, it is likely to assume that in the system under study the aquods solution is saturated with nanotubes. Because no interaction between CTAB and PVP appears to exist, and SWNTs and PVP have distinct hydrophilicities (resulting in extremely weak van der Waals interactions between SWNTs and PVP), the increase on SWNT dispersion triggered by the presence of PVP in the CTAB/ SWNT system is likely through a physical mechanism similar to the one proposed by Granite and collaborators. In this mechanism, the polymer is mainly occupying space in solution and sterically stabilizing nanotubes [17].

Preliminary calculations were done to assess whether the polymer content was high enough to provide such an effect.

This was done by comparing the total available surface area of nanotubes in solution with the total projectable polymer area onto the nanotubes surface assuming the nanotubes as rigid cylinders, the PVP polymer as rigid spheres and their dimensions remaining constant throughout the solution. The maximum available area of SWNTs in solution was calculated assuming it to be a rigid cylinder with an average length of 500 nm, and a radius of 0.75 nm (as obtained through AFM (Table 4)). The area value obtained for a rigid nanotube of these dimensions was then multiplied by Avogadro's number and divided by the nanotube molecular weight, calculated as 750,000 g/mol for a 500 nm length, 0.75 nm in diameter nanotube assuming pure carbon, notice the molecular weight value obtained by GPC (Table 2) is close to the calculated value within a 15% error. This value (total available nanotube area/gram of nanotube in suspension) was then multiplied by the nanotube concentration in suspension, using again the concentration value obtained by GPC (Table 2) to obtain the total area of nanotube in the CTAB/PVP suspension.

The projectable area available from the polymer was calculated using the PVP hydrodynamic radius values obtained from GPC (Table 1) and treating the polymer in suspension as a sphere. This value was again multiplied by Avogadro's number and divided by the polymer molecular weight. The values obtained were then multiplied by the polymer concentration in solution. Then the total projectable area of polymer available in solution was divided by the total area of nanotubes available to obtain a polymer/nanotube area ratio. The obtained values are reported in Table 5. From a quick inspection of this table, it is clear that under the polymer concentrations tested in this study, the polymer can present a relatively large excess area to interact to the nanotube surface. This suggests that the surface of nanotube is likely covered with PVP.

To further explore this possibility, the data shown in Figure 4 was replotted as a function of the total projectable area of polymer reported in Table 3. The results obtained are shown in Figure 6. Comparing this Figure with the plot shown in Fig. 4, the results are quite similar: PVP 10 again is the most effective polymer for nanotube dispersion. This result supports the premise of the observed improvement on nanotube dispersion being the result of steric interactions. To refine this hypothesis, the issues associated with the contact mechanics between the polymer and the nanotube were explored. Smith and collaborators have also explored the ability of PVP to stabilize hydrophobic nanoparticles in aqueous solutions [39]. They used PVP of different molecular weights: 10,000 g/mol, 40,000 g/mol, 360,000 g/mol, and 2,500,000 g/mol to disperse polystyrene nanoparticles. Their report indicates that dispersions were only stable with PVP of molecular weight 40,000 g/mol or greater and only if the polymer completely covered the surface of the polystyrene nanoparticles. The authors stated that full coverage was critical to generate steric repulsions between the adsorbed polymer layers and thus stabilize the polymer aqueous suspensions. Nativ-Roth and coworkers reached similar conclusions when studying the interaction

mechanism of physically adsorbed block polymers over carbon nanotubes in aqueous suspensions. They reported that a minimum of 20 monomeric units of polyethylene-oxide (PEO) were necessary in a PEO-polydimethylsiloxane-PEO triblock polymer for SWNT to be sterically driven apart to a stable separation distance [40].

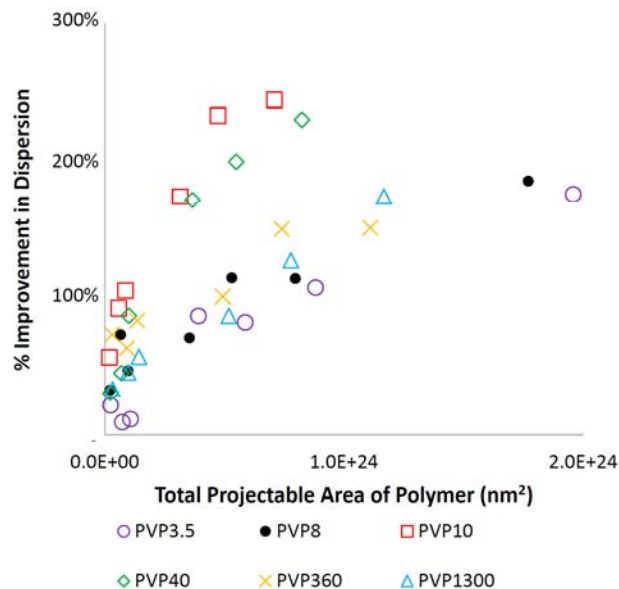


Figure 6. Percentage on improvement in dispersion respect to CTAB alone observed on SWNT suspensions prepared using 0.1% wt/vol CTAB and PVP of different molecular weights (\circ PVP 3,500; \bullet PVP 8,000; \square PVP 10,000; \diamond PVP 40,000; \times PVP 360,000; \triangle PVP 1,300,000) at different concentrations as a function of total projectable area of polymer.

The values for hydrodynamic diameters obtained by GPC for the different PVP samples, presented in Table 1, indicate PVP 10 has a hydrodynamic radius of 2.4 nm which is very close to the required intertube minimum separation distance of 2.5 nm reported as needed to achieve effective SWNT dispersions in aqueous systems [38]. At the same time PVP 3.5 and PVP 8, which have smaller hydrodynamic radii (1.4 and 1.9 nm respectively) are less effective as nanotube dispersant. Thus experimental results thus suggest the PVP macromolecule should have a hydrodynamic radius approximately the same size as the minimum intertube distance for nanotubes to be effectively dispersed. This however indicates that PVP 10 (hydrodynamic radius 2.5 nm) would provide a total separation distance of approximately 5 nm between each nanotube (assuming PVP in solution as rigid spheres). This is twice as large as the critical minimum intertube distance reported. However, for the case on SWNT aqueous suspensions using Gum Arabic (GA), stabilization is achieved only at a distance twice the polymer radius of gyration (1.54 times the hydrodynamic radius for a random coil Gum Arabic polymer) [41].

Although this model may explain why PVP 3.5 and PVP 8 are ineffective, compared to PVP 10, it does not provide a rationale for why PVP 360 and PVP 1300 are also ineffective. Hence a model based only on polymer rigid spheres does not seem to be able to fully explain the

experimental trends observed. Thus, this model was refined by exploring the mechanics of interaction between SWNTs and PVP. This was achieved by calculating, their common contact area, as given by a geometrically simplified Hertzian model [42]. In this simplified version of the Hertzian model, the tridimensional complexity is reduced to one dimension by considering the area of the polymer in contact with the nanotube as a circle penetrating an elastic surface. This is given by the formula below:

$$A = a^2\pi = Rd\pi \quad (2)$$

Where A represents the contact area, a the contact radius, d the depth of penetration and R the radius of the indenter. This model thus has the contact area as proportional to the polymer radius. Notice that the calculated values are different from that obtained using a “projectable area” where all the polymer outer surface is assumed to be in contact with the nanotube. The contact area model was therefore used to get a better description of the system. CTAB and PVP do not significantly interact with each other thus particular attention was focused on the PVP/SWNT interaction. To simplify the system further the following assumptions were made: the depth of penetration is relatively small (respect to the polymer radius) and constant across all polymer molecular weights, since it was assumed the nanotube walls are rigid. The depth of indentation was arbitrarily set as 0.1 nm across all calculations whereas the polymer hydrodynamic radius is used as the radius of the indenter. This simplification permits comparison of contact areas in the PVP system at different polymer molecular weights. The calculation thus converts absolute polymer concentrations into “amount of available polymer area in contact with nanotubes in suspension”. To obtain this value the moles available of polymer in suspension was multiplied by the polymer contact area (A) for all range of concentrations and PVP molecular weights tested in this study. The data shown in Figure 4 was replotted using these calculated values. The results are shown in Figure 7.

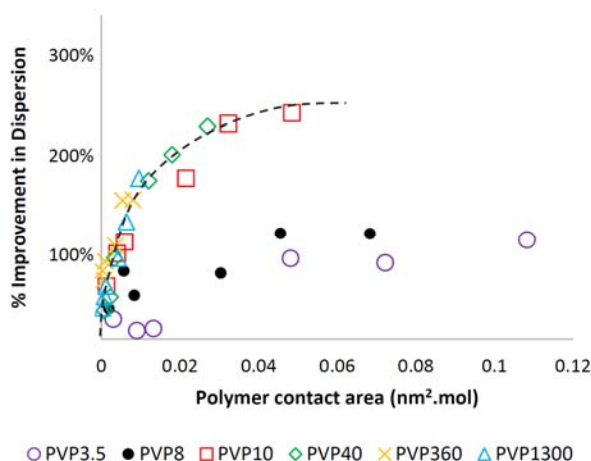


Figure 7. Percentage on improvement in dispersion respect to CTAB alone observed on SWNT suspensions prepared using 0.1% wt/vol CTAB and PVP of different molecular weights (\circ PVP 3,500; \bullet PVP 8,000; \square PVP 10,000; \diamond PVP 40,000; \times PVP 360,000; \triangle PVP 1,300,000) at different concentrations as a function of polymer contact area as obtained using a simplified Hertzian model.

Interestingly, unlike the previous plots (Figs. 4 and 6) the trends obtained for four out of the six samples (PVP 10, PVP 40, PVP 360 and PVP 1300) shift and align. This result, once again, strongly suggests that the quality of the SWNT dispersion obtained using different molecular weights of PVP is linked to the polymer hydrodynamic radii. PVP 3.5 and PVP 8 remain as poor dispersing agents presumably because of its small size (as discussed above, their hydrodynamic radius does not meet the minimum intertube distance required for effective SWNT dispersion). Hence it is proposed that PVP 360 and PVP 1300 disperse nanotubes based on the same mechanism as PVP 10 and PVP 40. The reason why PVP 360 and PVP 1300 appeared as poor dispersed agents compared to PVP 10 and PVP 40 when dispersion quality is plotted as function of total polymer mass concentration (Fig. 3) is because at any specific mass concentration, the number of large molecular weight polymers in solution will always be a lot lower than that of smaller polymer given their differences in weight. Thus, when everything is standardized based on contact area, the dispersion profiles of PVP (for PVP with molecular weight equal or above 10,000 g/mol) become independent of molecular weight and are solely a function of concentration.

5. Conclusion

Based on detailed spectroscopic and physiochemical analysis it is proposed that the synergistic effect observed in the CTAB-PVP system for SWNT dispersion is due to a physical mechanism in which the effective polymer contact area with the suspended nanotube, rather than the polymer molecular weight regulates PVP ability for SWNT dispersion. The role of CTAB seems to be confined to acting as interphase between the hydrophobic nanotube wall and the aqueous environment. These two effects thus suggest that steric interactions play a fundamental role on the stability of these nanotube suspensions.

Acknowledgements

The authors thank Profs. Amarjeet Bassi, Lars Rehmann, and John R. de Bruyn at Western University for allowing them to use their research equipment. The financial support from the Natural Sciences and Engineering Research Council of Canada, and Canadian Foundation for Innovation is also gratefully acknowledged.

References

- [1] K. Soma, T. K. Radhakrishnan, and J. Sarat Chandra Babu, “Carbon nanotubes: Their role in engineering applications and challenges ahead” *Inorganic and Nano-Metal Chemistry* vol. 47, pp. 188-196, 2017.
- [2] M. M. Shulaker, H. Wei, S. Mitra, and H. S. P. Wong, “Carbon Nanotubes for Monolithic 3 D ICs” in *Carbon Nanotubes for Interconnects, Process, Design and Applications*, A. Todri-Sanial, J. Dijon, and A. Maffucci, Springer International Publishing, Switzerland, 2017, pp. 315-333.

- [3] L. Feng, K. Li, B. Xue, Q. Fu, and L. Zhang, "Optimizing matrix and fiber/matrix interface to achieve combination of strength, ductility and toughness in carbon nanotube-reinforced carbon/carbon composites", *Materials & Design*, vol. 113, pp. 9-16, 2017.
- [4] M. I. Sajid, U. Jamshaid, T. Jamshaid, N. Zafar, H. Fessi, and A. Elaissari, "Carbon nanotubes from synthesis to in vivo biomedical applications, *International Journal of Pharmaceutics*", *International Journal of Pharmaceutics*, vol. 501, pp. 278-299, 2016.
- [5] Z. Zhuang, S. A. Giles, J. Zheng, G. R. Jenness, S. Caratzoulas, D. G. Vlachos, and Y. Yan, "Nickel supported on nitrogen-doped carbon nanotubes as hydrogen oxidation reaction catalyst in alkaline electrolyte" *Nature communications* vol. 7, 2016.
- [6] C. J. Shih, S. Lin, M. S. Strano, and D. Blankschtein, "Understanding the stabilization of single-walled carbon nanotubes and graphene in ionic surfactant aqueous solutions: large-scale coarse-grained molecular dynamics simulation-assisted DLVO theory." *Journal of Physical Chemistry C* vol. 119, pp. 1047-1060, 2015.
- [7] Y. Tan, and D. E. Resasco, "Dispersion of single-walled carbon nanotubes of narrow diameter distribution" *Journal of Physical Chemistry B* vol. 109, pp. 144541 4460, 2005.
- [8] N. Nakashima, and T. Shiraki, "Solubilisation technologies of carbon nanotubes", *International Polymer Science and Technology*, vol. 43, T 1, 2016.
- [9] V. C. Moore, M. S. Strano, E. H. Haroz, R. H. Hauge, R. E. Smalley, J. Schmidt, and Y. Talmon, "Individually Suspended Single-Walled Carbon Nanotubes in Various Surfactants" *Nanoletters* vol. 3, pp. 1379-1382, 2003.
- [10] L. Jiang, L. Gao, and J. Sun, "Production of aqueous colloidal dispersions of carbon nanotubes" *J. Colloid Interface Sci.* vol. 260, pp. 89-94, 2003.
- [11] K. Yurekli, C. A. Mitchell, and R. Krishnamoorti, "Small-Angle Neutron Scattering from Surfactant-Assisted Aqueous Dispersions of Carbon Nanotubes" *J. Am. Chem. Soc.* Vol. 126, pp. 9902-9903, 2004.
- [12] S. K. Samanta, M. Fritsch, U. Scherf, W. Gomulya, S. Z. Bisri, and M. A. Loi, "Conjugated polymer-assisted dispersion of single-wall carbon nanotubes: the power of polymer wrapping", *Accounts of chemical research* vol. 47, pp. 2446-2456, 2014.
- [13] M. J. O'Connell, P. Boul, L. M. Ericson, C. Huffman, Y. Wang, E. Haroz, and R. E. Smalley, "Reversible water-solubilization of single-walled carbon nanotubes by polymer wrapping", *Chem. Phys. Lett.* vol. 342, pp. 265-271, 2001.
- [14] A. Maity, S. Sinha Ray, and M. J. Hato, "The bulk polymerisation of N-vinylcarbazole in the presence of both multi- and single-walled carbon nanotubes: A comparative study", *Polymer* vol. 49, pp. 2857-2865, 2008.
- [15] M. Zheng, A. Jagota, E. D. Semke, B. A. Diner, R. S. Mclean, S. R. Lustig, R. E. Richardson, and N. G. Tassi, "DNA-assisted dispersion and separation of carbon nanotubes", *Nat. Mater.* vol. 2, pp. 338-342, 2003.
- [16] Y. Dror, W. Pyckhout-Hintzen, and Y. Cohen, "Conformation of polymers dispersing single-walled carbon nanotubes in water: A small-angle neutron scattering study", *Macromolecules*, vol. 38, pp. 7828- 7836, 2005.
- [17] M. Granite, A. Radulescu, and Y. Cohen, "Small-angle neutron scattering from aqueous dispersions of single-walled carbon nanotubes with Pluronic F 127 and poly (vinylpyrrolidone)", *Langmuir* vol. 28.30, pp. 11025-11031, 2012.
- [18] I. Cotiuga, F. Picchioni, U. S. Agarwal, D. Wouters, J. Loos, and P. J. Lemstra, "Block - Copolymer - Assisted solubilization of carbon nanotubes and exfoliation monitoring through viscosity", *Macromolecular rapid communications* vol. 27, pp. 1073-1078, 2006.
- [19] K. Tsuchiya, K. Uchida, Y. Kaminosono, K., Shimizu, T. Ishii, and H. Yajima, "High purity and yield separation of semiconducting single-walled carbon nanotubes dispersed in aqueous solutions with density gradient ultracentrifugation using mixed dispersants of polysaccharides and surfactants", *Japanese Journal of Applied Physics*, vol 52 (3 R), pp. 035102, 2013.
- [20] J. Ning, J. Zhang, Y. Pan, and J. Guo, "Surfactants assisted processing of carbon nanotube-reinforced SiO₂ matrix composites" *Ceramics International*, vol. 30, pp. 63-67, 2004.
- [21] T. J. Davis, and J. E. Herrera, "The Role of Single Walled Carbon Nanotube Debundling on Their Effective Reinforcement of Chitosan-Polyvinylpyrrolidone Hydrogels" *JNAN* vol. 5, pp. 247-254, 2015.
- [22] J. J. Filliben, and J. E. McKinney, "Confidence limits for the abscissa of intersection of two linear regressions ", *National Bureau of Standards*, 1972.
- [23] M. J. O'Connell, S. M. Bachilo, C. B. Huffman, V. C. Moore, M. S. Strano, E. H. Haroz, K. L. Rialon, P. J. Boul, W. H. Noon, C. Kittrell, J. Ma, R. H. Hauge, R. B. Weisman, and R. E. Smalley, "Band gap fluorescence from individual single-walled carbon nanotubes", *Science* vol. 297, pp. 593-596, 2002.
- [24] C. Clasen, J. P. Plog, W-M. Kulicke, M. Owens, C. Macosko, L. E. Scriven, M. Verani, and G. H. McKinley, "How dilute are dilute solutions in extensional flows?," *Journal of Rheology* vol. 50, pp. 849-881, 2006.
- [25] W. W. Graessley, "Polymer chain dimensions and the dependence of viscoelastic properties on concentration, molecular weight and solvent power", *Polymer* vol. 21, pp. 258-262, 1980.
- [26] D. P. Norwood, E. Minatti, and W. F. Reed, "Surfactant/polymer assemblies. 1. Surfactant binding properties." *Macromolecules* vol. 31, pp. 2957-2965, 1998.
- [27] J. Desbrieres, R. Borsali, M. Rinaudo, and M. Milas, "chi-F Interaction parameter and the single-chain diffusion coefficients of dextran/poly (vinylpyrrolidone)/water: dynamic light scattering experiments." *Macromolecules* vol. 26, pp. 2592-2596, 1993.
- [28] Y. Kim, and H. Kim, "Effect of extensional properties of polymer solutions on the droplet formation via ultrasonic atomization", *Polym. Eng. Sci.* vol. 51, pp. 2446-2452, 2011.
- [29] J. Hilding, E. A. Grulke, Z. G. Zhang, and F. Lockwood, "Dispersion of carbon nanotubes in liquids", *J. Dispers. Sci. Technol.* Vol. 24, pp. 1-41, 2003.
- [30] A. J. Blanch, C. E. Lenehan, and J. S. Quinton, "Parametric analysis of sonication and centrifugation variables for dispersion of single walled carbon nanotubes in aqueous solutions of sodium dodecylbenzene sulfonate", *Carbon* vol. 49, pp. 5213-5228, 2011.

- [31] V. G. Hadjiev, M. N. Iliev, S. Arepalli, P. Nikolaev, and B. S. Files, "Raman scattering test of single-wall carbon nanotube composites" *Applied Physics Letters*, vol. 78, pp. 3193-3195, 2001.
- [32] D. A. Heller, R. M. Mayrhofer, S. Baik, Y. V. Grinkova, M. L. Usrey, and M. S. Strano "Concomitant length and diameter separation of single-walled carbon nanotubes", *J. Am. Chem. Soc.* Vol. 126, pp. 14567-14573, 2004.
- [33] M. F. Islam, E. Rojas, D. M. Bergey, A. T. Johnson, and A. G. Yodh, "High weight fraction surfactant solubilization of single-wall carbon nanotubes in water", *Nano Lett.* vol. 3, pp. 269-273, 2003.
- [34] K. Shirahama, K. Mukae, and H. A. Iseki, "A cationic surfactant is bound to poly (vinylpyrrolidone) in high pH media" *Colloid Polym. Sci.* vol. 272, pp. 493-496, 1994.
- [35] G. Wang, and G. Olofsson, "Titration calorimetric study of the interaction between ionic surfactants and uncharged polymers in aqueous solution" *J. Phys. Chem. B* vol. 102, pp. 9276-9283, 1998.
- [36] R. Bury, B. Desmazières, and C. Treiner, "Interactions between poly (vinylpyrrolidone) and ionic surfactants at various solid/water interfaces: a calorimetric investigation" *Colloids Surf. Physicochem. Eng. Asp.* vol. 127, pp. 113-124, 1997.
- [37] Y. Feng, X. W. Fang, S. Z. Mao, S. Zhao, H. Z., Yuan, J. Y. Yu, and R. Y. Du, "Interaction of poly (vinylpyrrolidone) with cationic and nonionic surfactants in aqueous solution studied by ^1H NMR", *Colloid Polym. Sci.* vol. 281, pp. 902-906, 2003.
- [38] X. Qi, P. Wang, L. Ji, X. Tan, and L. Ouyang, "Dispersion of carbon nanotubes in aqueous solution with cationic surfactant CTAB", *J. Inorg. Mater.* vol. 22, pp. 1122-1126, 2007.
- [39] J. N. Smith, J. Meadows, and P. A. Williams, "Adsorption of polyvinylpyrrolidone onto polystyrene lattices and the effect on colloid stability", *Langmuir* vol. 12, pp. 3773-3778, 1996.
- [40] E. Nativ-Roth, R. Shvartzman-Cohen, C. Bounioux, M. Florent, D. Zhang, I. Szleifer, and R. Yerushalmi-Rozen, "Physical adsorption of block copolymers to SWNT and MWNT: A nonwrapping mechanism", *Macromolecules* vol. 40, pp. 3676-3685, 2007.
- [41] R. Bandyopadhyaya, E. Nativ-Roth, O. Regev, and R. Yerushalmi-Rozen, "Stabilization of individual carbon nanotubes in aqueous solutions," *Nanoletters*, vol. 2, pp. 25-28, 2002.
- [42] T. Geike, and V. L. Popov, "Mapping of three-dimensional contact problems into one dimension", *Phys. Rev.* vol. E 76, pp. 036710, 2007.